

Probing the local field of nanoantennas using single particle luminescence

A. L. Lereu,¹ G. Sanchez-Mosteiro,¹ P. Ghenuche,¹ A. Passian,²
R. Quidant,^{1,4} M. Garcia-Parajo,^{3,4} N. F. van Hulst^{1,4}

¹ ICFO - Institut de Ciències Fotòniques, 08860 Castelldefels (Barcelona), Spain

² Oak Ridge National Laboratory, Oak Ridge, Tennessee 37831, USA

³ IBEC - Institut de Bioenginyeria de Catalunya & CIBER, 08028 Barcelona, Spain

⁴ ICREA - Institutio Catalana de Recerca i Estudis Avançats, 08015 Barcelona, Spain

E-mail: aude.lereu@icfo.es

Abstract. Intense local fields bound to the surface of engineered metallic nanostructures are currently of a great interest for many applications including enhanced imaging, spectroscopy, sensing or lab-on-a-chip devices. Their resonance characteristics can be tuned by the size, shape, incident optical frequency and polarization state. We present here an investigation of the local field of gold dimers manufactured in an array. Finally, employing retarded electrodynamics, we computationally visualize the field distribution and obtain the spectral response of a unique dimer.

1. Introduction

Metallic nanoparticles are the subject of intense investigations particularly in sensing and in lab-on-a-chip devices. The development of fabrication techniques such as electron-beam lithography or focused ion beam [1]-[3], has also profited the explosion of the field. An interesting behavior of nanoparticles is their tunable spectral response that may be modified as a function of size, shape or material [4, 5], and in this sense diverse nanoparticles are commonly made and explored [6]-[11].

We previously investigated gold dimer structures by near field optical microscopy [12] as well as two-photon luminescence (TPL) [13]. In the near field microscopy, a depolarization effect of the electric field was observed associated with an enhancement of the near field probe brightness. In the TPL measurements, an enhancement factor of 10 was reported for a separation of 30 nm between the two particles constituting the dimer. In this paper, we investigate the luminescence of individual dimers and monomers by means of confocal microscopy (see Section 2), and provide statistics of the effects. We look into polarization comparisons for two cases of separation distances. Spectroscopy studies are carried out both experimentally and theoretically, and the electric field amplitude is numerically computed in order to get some understanding on the resonance behavior of such a structure, as seen in Section 3. A conclusion is gathered in Section 4.

2. Experiment

We investigate the luminescence of individual gold nano-structures designed as a continuation of 3 lines of dimers, and 2 lines of single particles; i.e. monomers (see insets (a & b) Fig. 1). Arrays of such structures were fabricated, in matrices of $100\ \mu\text{m} \times 100\ \mu\text{m}$, with a period of $1\ \mu\text{m}$, by standard electron-beam lithography and thin film evaporations. More details on the fabrication process can be found in the references section [13]. The manufactured gold (Au) dimers are composed of two monomers with a diameter of $100\ \text{nm}$ and a height of $40\ \text{nm}$, that are either touching, i.e. separated by a “gap of $0\ \text{nm}$ ”, or are distant by a gap of $30\ \text{nm}$.

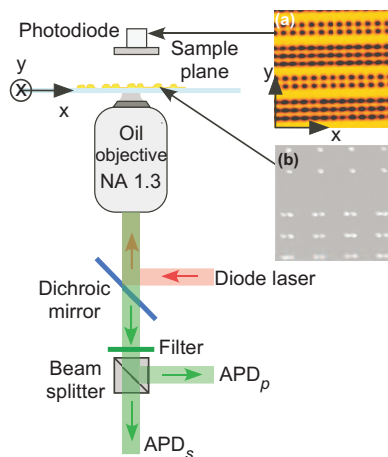


Figure 1. Confocal microscope with single molecule detection scheme. The sample is scanned in xy -plane with piezoelectric elements linked to the feedback controller. A laser light is brought to the sample via a high numerical aperture objective, and the reflected luminescence from the sample is collected through the same objective. Two avalanche photodiodes are detecting two orthogonal polarization components. Simultaneously a photodiode, positioned above the sample, collects the transmitted field [inset (a)] permitting to localize the dimers and monomers. A scanning electron beam image of the sample is given in the inset (b).

In our experimental setup, described in Fig. 1, a scanning confocal microscope with a high numerical aperture objective (NA 1.3, 100x), which is typically associated with single molecule detection, was used. One optical path of the confocal microscope is used to excite the structures utilizing a diode laser with a wavelength $\lambda = 635\ \text{nm}$ and a power density of approximately $34\ \text{kW}/\text{cm}^2$. The diode laser is linearly polarized and controlled via a $\lambda/2$ waveplate. The second optical path of the microscope, after hitting the sample plane and therefore resulting from the luminescence of the individual gold structures, is collected in reflection through the objective and separated from the illumination light by a dichroic mirror and a long pass filter assembly. After filtering, the reflected light is directed to the detection site, which is composed of a polarizing beam splitter and two avalanche photodiodes. This detection method allows the decomposition of the luminescence into two orthogonal polarization components and therefore permits access to a polarization information often hidden in different nanostructured systems.

3. Results and discussion

Scattering spectroscopy of the structure is first measured, see graph of Fig. 4, showing a peak near $634\ \text{nm}$ for the p polarization, justifying our choice of the excitation wavelength. A comparison with the computational model for the field distribution and spectral response of individual dimers is also given which shows agreements in term of peak localization.

Using confocal measurements, we investigated polarization effects on dimers, for the two separation gaps: $30\ \text{nm}$ gap in Fig. 2 and no-gap in Fig.3. We compare the luminescence response as the polarization excitation is rotated from p (parallel to the dimers axis); referred to Figs. 2a) & 3 a); to s (perpendicular to the dimers axis); referred to Figs. 2b) & 3 b). For each excitation state, we collect simultaneously two images via the APD_p and APD_s (see Fig. 1), detecting respectively the p - and s -polarized luminescence response of the structures. The two obtained images are superimposed and results in the images of Figs. 2 & 3 for a scan area of

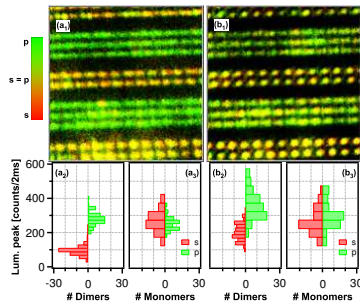


Figure 2. Resonance case: Luminescence measurements of single gold dimers with a gap of 30 nm. Figures (a) and (b) illustrates the luminescence of the structures when illuminated with long-axis polarized excitation light and with short-axis polarized one, respectively. (a_1 & b_1) Luminescence image of a $10 \times 10 \mu\text{m}$ scanned area. The color scale gives the polarization state of the detected field. (a_2 & b_2) and (a_3 & b_3) Distribution of the luminescence peak for dimers and monomers respectively.

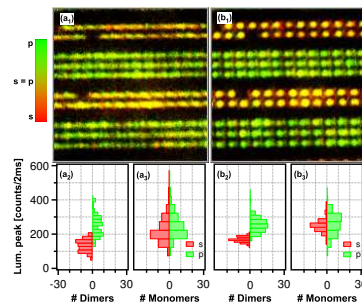


Figure 3. Non-resonance case: Luminescence measurements of single gold dimers with no-gap. Figures (a) and (b) demonstrate the different excitation polarizations. (a_1 & b_1) Luminescence image of a $10 \times 10 \mu\text{m}$ scanned area. The color scale gives the polarization state of the detected field. (a_2 & b_2) and (a_3 & b_3) Distribution of the luminescence peak for dimers and monomers respectively.

$10 \mu\text{m} \times 10 \mu\text{m}$. The color scale represents the polarization state of the collected photons going from *red* for “pure” *s* to *green* for “pure” *p*. The *yellow* denotes an equal contribution from both polarizations. At a first glance, we can conclude that, thanks to the symmetry of the monomers, they exhibit, as expected, a response with equal amounts of *p* and *s* polarizations, whereas the dimers possess a response mainly *p*-polarized. In order to quantify the phenomenon, statistical studies of the polarization effect on the luminescence of individual particles were carried out from the confocal images. Monomers were simultaneously investigated in order to have a true reference and to eliminate potential discussions concerning substrate effects.

We first extract, from Figs. 2 & 3, the statistics of the intensity peaks of luminescence for both *p* and *s* polarizations, depicted in Figs. 2 & 3 a_2) & b_2) for the dimers and in Figs. 2 & 3 a_3) & b_3) for the monomers. Broad distributions are seen from dimers to dimers as well as from monomers to monomers. This may be explained on the basis of the variations in the fabrication process, inducing uncertainties in the shape and size of each particle, and from roughness issues. For the two considered gap sizes, a shift in the luminescence distribution is observed between the detected *p*-polarized signal and the *s*-polarized one, where the *p*-polarized luminescence is, for both gaps, stronger than the *s* one. This is to be expected as the localized plasmon excitation is engaged in this process, provoking resonant modes excitation. For a 30 nm gap, a *p*-polarized excitation should install a strong coupling between the local charges of the gold particles, whereas the *s* polarization would excite independently local charges of each single particle constituting the dimer. This is shown in Fig. 4a) to c) representing the electric field amplitude in the near field of the nanostructures. For the no-gap situation, the same observation is still valid, however, the effect is much less. This observation is foreseen as the particles do not couple with each other but act as a unique elongated particle.

We then extrapolate the polarization ratio, from the intensity peaks of luminescence, meaning the ratio between the *p*-polarized luminescence and the *s*-polarized one, illustrated in Fig. 5a) for the 30 nm gap and b) for no-gap. This leads to an average ratio, recapitulated in Table 1 for

Table 1. Polarization ratios as a function of gap size and excitation polarization

- Gap size	Polarization	
	p	s
30 nm	3.10	1.60
0 nm	1.80	1.40

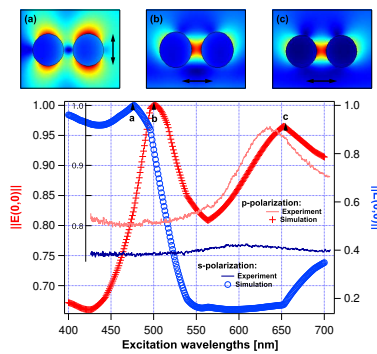


Figure 4. Theoretical and experimental spectroscopy of the electric field amplitude for dimers with 30 nm gap. The insets (a) to (c) portray the total field fingerprint for each marked theoretical peak, to illustrate the envisaged resonances and field enhancement due to the metallic structures.

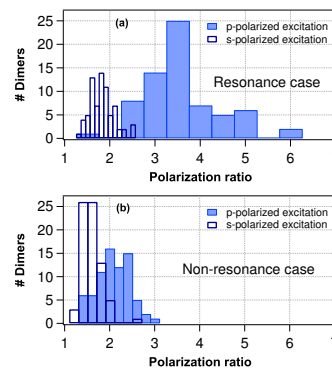


Figure 5. Distribution of the detected polarization ratio (p polarization over s polarization) for the dimers. (a) represents the resonance case (30 nm gap) and (b) the non-resonance case with no-gap.

both gap sizes and polarization excitations, and we compare to the monomers case that is, as envisaged, close to unity. An averaged enhancement factor of 3 is hence shown with respect to the monomers for the right geometric and excitation conditions. A weaker increase observed for the non-resonance case with p -polarized excitation may be attributed to the elongated shape of the dimers. For s -polarized excitation, no noticeable difference is seen with respect to gap sizes, that is the two particles act as two independent dipoles. This statement is reinforced by the actual measured values close to 1 in the s -polarization, approaching the monomers behavior.

4. Conclusion

Collective behavior of gold dimers was reported in large arrays, realized by electron-beam lithography. We demonstrate the polarized behavior of such structures where a polarization ratio enhancement was observed in the resonance case. A factor of 3 is reported with respect to the monomers isotropic response, in agreement with the previous work [13] on similar structures, measuring TPL, where a factor of 10 in intensity was found. In addition, a maximum polarization ratio of 6 was observed, following the factor of 100 observed in [3] by TPL for bowtie structures. A comparison between spectroscopic measurement and the computed absorption of an individual dimer was made and showed some agreements in the case of p polarization. Understanding the local field of metallic nanostructures should lead to improvements of their use in sensing or spectroscopy application. The next step being to implement the capability of positioning the substance of interest in the right place with respect to the metallic structure.

Acknowledgement

This work benefits from the financial support of the Specific Target Research Project (STRP) ASPRINT and the NoE PlasmO-Nano-Devices in the 6th Framework Program of the European Community. This work was also funded by ATOM3D (FP6-508952), PhOREMOST (FP6-511616), TIC2003-07485, and MOCA (TIC 2003-01038).

References

- [1] Ito T and Okazaki S 2000 *Nature* **406** 1027
- [2] Haynes C L and van Duyne R P 2001 *J. Phys. Chem. B* **105** 5599
- [3] Mühlischlegel P, Eisler H -J, Martin O J F, Hecht B and Pohl D W 2005 *Science* **308** 1607
- [4] Keilmann F 1999 *J. Microsc.* **194** 567
- [5] Matteo J A and Hesselink L 2005 *Optics Express* **13** 636
- [6] Girard C and Dujardin E 2006 *J. Opt. A: Pure Appl. Opt.* **8** S73
- [7] Girard C 2005 *Rep. Prog. Phys.* **68** 1883
- [8] Tamaru H, Kuwata H, Miyazaki H T and Miyano K 2002 *Appl. Phys. Lett.* **80** 1826
- [9] Enoch S, Quidant R and Badenes G, 2004 *Opt. Express* **12** 3422
- [10] Ghenuche P, Quidant R and Badenes G, 2005 *Opt. Lett.* **30** 1882
- [11] Talley C E, Jackson J B, Oubre C, Grady N K, Hollars C W, Lane S M, Huser T R, Nordlander P and Halas N J 2005 *Nanoletters* **5** 1569
- [12] Lereu A L, Sanchez-Mosteiro G, Ghenuche P, Quidant R and van Hulst N F 2007 *J. Microscopy*
- [13] ten Bloemendal D, Ghenuche P, Quidant R, Cormack I G, Loza-Alvarez P and Badenes G 2006 *Plasmonics* **1** 41